Journal of the Korean Physical Society, Vol. 69, No. 4, August 2016, pp. 573∼577

The Hybridizations of Cobalt 3d Bands with the Electron Band Structure of the Graphene/Cobalt Interface on a Tungsten Substrate

Jinwoong Hwang* and Choongyu Hwang†
Department of Physics, Pusan National University, Busan 46241, Korea

Nak-Kwan Chung*
Vacuum Center, Korea Research Institute of Standards and Science, Daejeon 34113, Korea

A. D. N'Diaye and A. K. Schmid
National Center for Electron Microscopy, Lawrence Berkeley National Laboratory, Berkeley, CA 94720, USA

Jonathan Denlinger
Advanced Light Source, Lawrence Berkeley National Laboratory, Berkeley, CA 94720, USA

(Received 5 July 2016, in final form 11 July 2016)

The interface between graphene and a ferromagnetic substrate has attracted recent research interests due to its potential for spintronic applications. We report an angle-resolved photoemission spectroscopy study on the interface between graphene and cobalt epitaxially grown on a tungsten substrate. We find that the electron band structure of the interface exhibits clear discontinuities at the crossing points with cobalt 3d bands. These observations indicate strong hybridizations between the electronic states in the interface and provide an important clue to understand the intriguing electromagnetic properties of the graphene/ferromagnet interface.

PACS numbers: 73.20.At, 73.22.Pr, 73.40.Ns
Keywords: Graphene, Cobalt, Interface, ARPES, Electron band structure
DOI: 10.3938/jkps.69.573

I. INTRODUCTION

The interface between graphene and a cobalt substrate allows graphene to possess intriguing physical properties that do not exist when graphene remains intact from the substrate. For example, spin-polarized low-energy electron microscopy experiments showed that upon covering a cobalt substrate with graphene, the magnetic asymmetry of the substrate was reversed [1], in line with an experimental result obtained using X-ray magnetic circular dichroism [2]. The observed antiparallel magnetic ordering of graphene with respect to the cobalt substrate has been attributed to the hybridization of the electron states in graphene and the substrate [1].

Angle-resolved photoemission spectroscopy (ARPES) studies, indeed, proved strong hybridization [3, 4] so that the conduction band of the graphene π bands is mostly blurred, consistent with a recent theoretical result [5]. Despite the hybridization, however, the crossing point between the conduction and valence bands of the π bands, observed at 2.8 eV below the Fermi energy, $E_{\rm F}$, remains intact, suggesting that the substrate-induced sublattice symmetry breaking does not only open an energy gap [6–8] but also possibly closes the gap [3]. The hybridization gives rise to spin polarization of the π bands [9] or induces another surprising magnetic property such as a single-spin mini Dirac cone near $E_{\rm F}$ [10].

Here, we used the ARPES technique to investigate further the electron band structure of the graphene/cobalt interface epitaxially grown on a tungsten substrate. We observed parabolic bands from the cobalt thin film and the tungsten substrate that showed discontinuities near $E_{\rm F}$. These spectral features are attributed to the interference or the hybridization between cobalt 3d bands and the electron band structure of the interface [11–13]. Near the Brillouin zone corner of the graphene unit cell, the strong hybridization between graphene π bands and cobalt 3d bands results in a mini Dirac cone [10]. We found that the electron band structure, possibly corresponding to a mini Dirac cone, persisted down to 0.54 eV below $E_{\rm F}$.

*These authors contributed equally to this work.
†E-mail: ckhwang@pusan.ac.kr

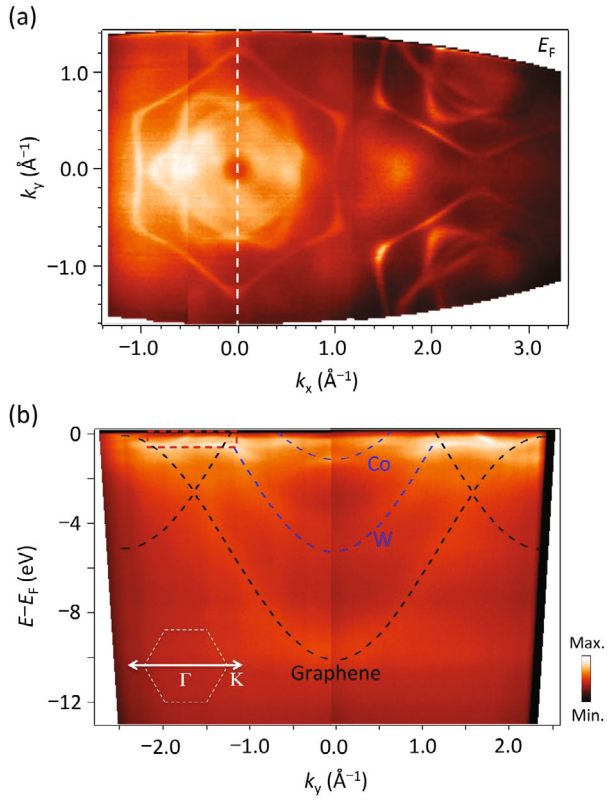

Fig. 1. (Color online) (a) Fermi surface of the graphene/cobalt interface on a tungsten substrate. (b) ARPES intensity map taken along the ΓK direction of the graphene unit cell as denoted by the white arrow and the hexagonal dashed lines, respectively, in the inset. Black dashed curves are graphene π bands calculated within the tight-binding formalism, and blue dashed curves are parabolic bands observed from the cobalt/tungsten substrate.

II. EXPERIMENTS

The graphene layer was prepared by using the chemical vapor deposition method [14] on 20 monolayers of a cobalt thin film on a W(110) substrate, as described elsewhere in detail [1]. The prepared sample was then transferred into an ultra-high vacuum, followed by a cleaning process using an e-beam heating method [15] up to a temperature of 630 °C, while the pressure was under 4×10^{-10} Torr. ARPES measurements have been performed at beamline 4.0.3 of the Advanced Light Source at Lawrence Berkeley National Laboratory. The sample was measured at 15 K with a photon energy and an energy resolution of 90 eV and 21 meV, respectively.

III. RESULTS AND DISCUSSION

Figure 1(a) shows the Fermi surface of the interface. The disk-like shape around the Γ point, *i.e.*, (k_x, k_y) = (0, 0), resembles that of quantum-well states confined in cobalt thin films [12]. The hexagonal feature enclosing the quantum-well states may originate from the tungsten substrate, which has been reported to be exposed when the cobalt thin films on the tungsten substrate is heated above 600 °C [13]. The electron band structure of graphene is not identified at E_F, consistent with a previous result [3]. To better understand the electron band structure of the interface, we show an ARPES intensity map in Fig. 1(b), along the white dashed line in Fig. 1(a) or the ΓK direction of the graphene unit cell as denoted by the white arrow in the inset of Fig. 1(b), where the white dashed hexagon denotes the graphene unite cell. The black dashed curves are calculated graphene π bands within the tight-binding formalism in the absence of the substrate. In a previous ARPES report [3], the crossing point between the conduction and the valence bands of the graphene π bands, the so-called Dirac energy E_D, was reported to be at 2.6 eV below E_F. Although the crossing point is not clearly observed in our data, the tight-binding bands are rigidly shifted towards higher binding energy; hence, the overall spectral shape roughly matches the experimental data at higher binding energies. In addition to the characteristic π bands of graphene, multiple parabolic bands centered at 0 Å^{-1} are observed at lower binding energies, as denoted by blue dashed curves. The lower parabolic band corresponds to the bulk *sp* band of tungsten [13] because, in a previous study, it was not observed from graphene on cobalt thin films grown on a W(110) substrate, but appeared when the cobalt films collapsed. The upper parabolic band near E_F is observed near the lowest energy of the quantum-well states [11] of cobalt thin films grown on a W(110) substrate [12]. The observation of both states suggest that due to the annealing process, cobalt atoms may exist as either thin films or islands between graphene and the tungsten substrate [13].

A zoomed-in view of the ARPES intensity map near E_F reveals the effect of cobalt 3*d* bands on these multiple parabolic bands. The blue dashed curves in Fig. 2(a) are the same parabolic bands drawn in Fig. 1(b). Figure 2(b) shows momentum distribution curves (MDCs), *i.e.*, photoelectron intensity spectra taken at constant energy as a function momentum, of the ARPES intensity map near E_F. When the black bars follow the local intensity maxima, each one approaches 0 Å^{-1} upon moving away from E_F, indicating the parabolic nature of both bands, in agreement with the inner and the outer blue dashed curves drawn in Fig. 2(a). Figures 2(c-d) and 2(e-f) present the outer and the inner parabolic bands, respectively, in a narrower momentum range. Figures 2(c) and 2(e) are ARPES intensity maps, and Figs. 2(d) and 2(f) are energy distribution curves (EDCs), *i.e.*, photoelectron intensity spectra taken at constant momentum as a function of $E - E_F$. The outer parabolic band shown in Figs. 2(c) and 2(d) exhibits clear discontinuities in both the spectral intensity and the energy-momentum dispersion (blue curves) at the crossing points with cobalt 3*d*

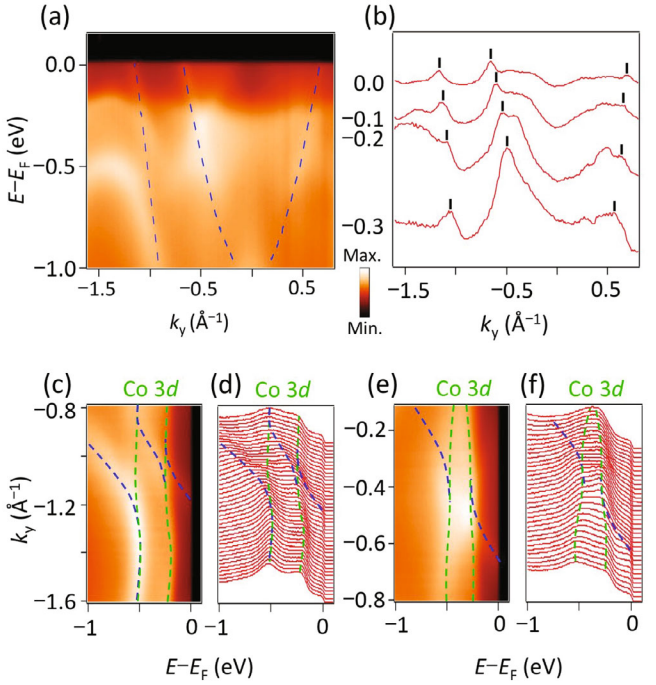

Fig. 2. (Color online) (a) ARPES intensity map near E_F taken along the ΓK direction of the graphene unit cell denoted in the inset of Fig. 1(b). (b) Momentum distribution curves at several different energies relative to E_F. Black bars follow the blue bands denoted in panel (a). (c-d) A zoomed-in view of the ARPES intensity map for the outer parabolic band (panel (c)) and energy distribution curves (panel (d)). Blue and green curves are the outer band and cobalt 3*d* bands, respectively. (e-f) A zoomed-in view of the ARPES intensity map for the inner band (panel (e)) and energy distribution curves (panel (f)). Blue and green curves are the inner band and cobalt 3*d* bands, respectively.

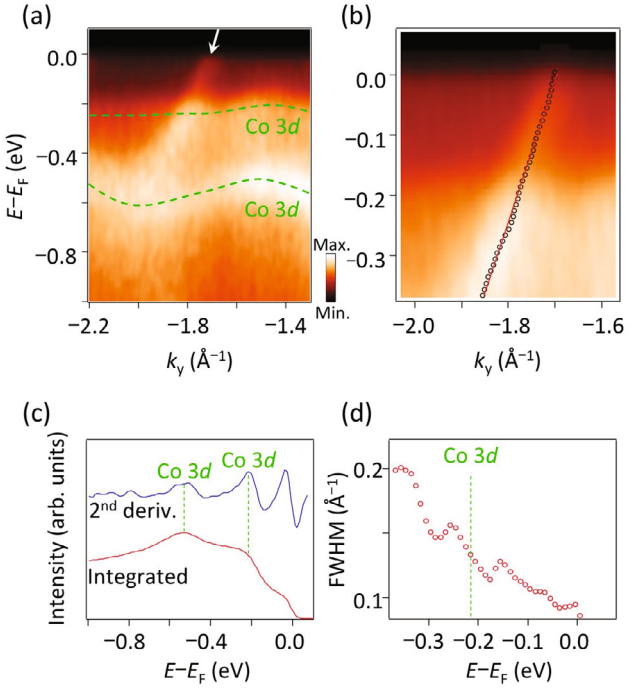

Fig. 3. (Color online) (a) ARPES intensity map near E_F and momentum of -1.7 Å^{-1} taken along the ΓK direction of the graphene unit cell. The green dashed curves are the cobalt 3*d* bands. (b) A zoomed-in view of near E_F. The black circles and the red solid line are a Lorentzian fit to the ARPES intensity map and an arbitrary straight line for a guide to the eyes. (c) Angle-integrated spectra (red curve) and its 2nd derivative (blue curve) for the ARPES intensity maps shown in panel (a). (d) Full width at half maximum of MDCs for the ARPES intensity maps shown in panel (b).

bands (green curves). When the outer band is a bulk state of the tungsten substrate [13], the discontinuities denote strong hybridizations [16] between cobalt overlayers and the tungsten substrate. The inner parabolic band also shows similar discontinuities at the crossing point with the cobalt 3*d* bands, as shown in Figs. 2(e) and 2(f). For the case of quantum-well states, such discontinuities have been attributed to the interference with the electrons from the substrate [11,17]; hence, the observation of such discontinuities in the graphene/cobalt interface might suggest an interference between the electrons from the quantum-well states and from the cobalt 3*d* bands within the cobalt thin film.

We have further investigated the electron band structure of the graphene/cobalt interface. Figure 3(a) shows an ARPES intensity map around $k_y = -1.7$ Å^{-1}, as denoted by the red dashed rectangle in Fig. 1(b). One can find a dispersive feature near E_F, as denoted by a white arrow, which becomes fuzzy below ~ -0.2 eV. This spectral feature is similar to that of the mini Dirac cone originating from hybridization between the conduction band of the graphene π bands and the cobalt 3*d* bands [10]. Interestingly, in a previous first-principles calculations in conjunction with spin-resolved ARPES measurements [10], this mini Dirac cone consists of a single spin, which is different from the conventional Dirac cone observed in graphene [18]. However, a clear difference in the observed band compared to the mini Dirac cone [10] is that only one of the branches of the mini Dirac cone is observed. This difference might originate from the photoemission matrix element effect. Typically, along the ΓK direction, the photoelectron intensity from one of the branches of the conical dispersion of graphene is completely suppressed, allowing us to measure only one branch for the valence band of the graphene π bands in the first Brillouin zone [19, 20]. In addition, this matrix element effect highly depends on the photon energy [21], resulting in an intensity variation between the two branches. Indeed, when we compare our work with a previous study, the photon energies are 50 eV and 28 eV, and the measurements are done parallel and perpendicular to the ΓK direction, respectively. Consequently, despite the matrix element effect for the mini Dirac cone of the graphene/cobalt interface [10] is not fully under-

stood yet, within the same analogy of understanding the photoelectron intensity from the Dirac cone of graphene, it might result in the absence of the photoelectron intensity for one of the branches of the mini Dirac cone in our result.

In a previous study [10], the energy spectrum of the mini Dirac cone was reported to be fuzzy below ~ -0.2 eV due to a hybridization with cobalt 3*d* bands. In our data, however, one can find that the spectral intensity of the measured dispersive band still persists below ~ -0.2 eV (although an enhanced background causes its spectral feature to be fuzzy) until it merges with a barely dispersive band at ~ -0.5 eV and vanishes beyond that energy. The latter energy is consistent with the cobalt 3*d* band with the higher binding energy shown in Figs. 2(c-f). Hence, the vanishing intensity of the dispersive band below ~ -0.5 eV indicates strong hybridizations of the observed band with the cobalt 3*d* band. To understand the detailed feature at the crossing point with the cobalt 3*d* band of the lower binding energy shown in Figs. 2(c-f), we extracted the energy-momentum dispersion from a Lorentzian fit to the band as shown in Fig. 3(b). While the red solid line is an arbitrary straight line for a guide to the eyes, the black circles are the fit result, and almost linear throughout the entire fitting range. To find the precise energy of the cobalt 3*d* bands, we show in Fig. 3(c) the second derivative (blue curve) of the angle-integrated intensity (red curve) of the ARPES intensity map shown in Fig. 3(a), providing binding energies of the cobalt 3*d* bands of 0.22 eV and 0.54 eV below E_{F}. The absence of any discontinuity at -0.22 eV in the fitted energy-momentum dispersion possibly suggests that the hybridization, if any, between mini Dirac cone and the cobalt 3*d* band with the lower binding energy is very weak. Indeed, the full width at half maximum of the MDCs does not show any abrupt change at 0.22 eV below E_{F}, as shown in Fig. 3(d), although a sharp increase is expected in the presence of hybridization between the two bands. Our result indicates that the energy scale of the dispersive band might be extended down to 0.54 eV below E_{F}.

Although the origin of the different energy scales of the mini Dirac cone and the dispersive band is not clear within our analysis, one of the differences between the previous and the current experiments is the sample growth temperature. The previous study [10] reported that the number of defects in graphene varied depending on the growth temperature. While the previous work was done at 660 °C [10], we used elevated temperatures of 600 °C – 800 °C, followed by an additional cleaning process at 630 °C. Different growth/cleaning conditions might have influenced not only the structural properties of the interface [13], as discussed in Fig. 1, but also the electronic properties via the presence of the defects. However, if the microscopic origin of the difference is to be understood, further theoretical and experimental investigations are invited.

IV. SUMMARY

We have investigated the electron band structure of a graphene interface with cobalt thin films epitaxially grown on a tungsten substrate. We found that cobalt 3*d* bands strongly influenced the electronic properties of the interface. The sample exhibited parabolic bands centered at the Γ point originating from quantum well states and the tungsten substrate. These bands showed clear discontinuities at the crossing points with cobalt 3*d* bands that were attributed to the interference between the electrons from the quantum-well states and the cobalt 3*d* bands and to the hybridization between the bulk *sp* band of the tungsten substrate and the cobalt 3*d* bands. The hybridization between graphene π bands and cobalt 3*d* bands results in additional spectral features near E_{F} similar to the mini Dirac cone observed in a previous ARPES study [10]. However, we found that this additional band persisted down to 0.54 eV below E_{F}, thus extending its energy scale compared to that of the mini Dirac cone reported in a previous study [10].

ACKNOWLEDGMENTS

This work was supported by a 2-Year Research Grant of Pusan National University.

REFERENCES

[1] A. T. N'Diaye and A. K. Schmid, Microsc. Microanal. **18**, 1538 (2012).
[2] H. Vita, St. Böttcher, P. Leicht, K. Horn, A. B. Stick and F. Máca, Phys. Rev. B **90**, 165432 (2014).
[3] A. Varykhalov, D. Marchenko, J. Sánchez-Barriga, M. R. Scholz, B. Verreck, B. Trauzettel, T. O. Wehling, C. Carbone and O. Rader, Phys. Rev. X **2**, 041017 (2012).
[4] D. Pacilé, S. Lisi, I. Di Bernardo, M. Papago, L. Ferrari, M. Disarray, M. Caputo, S. K. Mahatha, P. M. Sheverdyaeva, P. Moras, P. Lacovig, S. Lizzie, A. Baraldi, M. G. Betti and C. Carbone, Phys. Rev B **90**, 195446 (2014).
[5] G. Giovannetti, P. A. Khomyakov, G. Brocks, V. M. Karpan, J. van den Brink and P. J. Kelly, Phys. Rev. Lett. **101**, 026803 (2008).
[6] S. Y. Zhou, G. -H. Gweon, A. V. Fedorov, P. N. Firs, W. A. de Heer, D. -H. Lee, F. Guinea, A. H. Castro Neto and A. Lanzara Nat. Mater. **6**, 770 (2007).
[7] S. Kim, J. Ihm, H. J. Choi and Y. -W. Son, Phys. Rev. Lett. **100**, 176802 (2008).
[8] S. Kim, J. Ihm and Y. -W. Son, J. Korean Phys. Soc. **55**, 341 (2009).
[9] D. Marchenko, A. Varykhalov, J. Sánchez-Barriga, O. Rader, C. Carbone and G. Bihlmayer, Phys. Rev. B **91**, 235431 (2015).
[10] D. Usachov, A. Fedorov, M. M. Otrokov, A. Chikina, O. Vilkov, A. Petukho, A. G. Rybkin, Y. M. Koroteev, E.

V. Chulkov, V. K. Adamchuk, A. Grüneis, C. Laubschat and D. V. Vyalikh, Nano Lett. **15**, 2396 (2015).
[11] N. J. Speer, S. -J. Tang, T. Miller and T. -C. Chiang, Science **314**, 804 (2006).
[12] P. Moras, G. Bihlmayer, P. M. Sheverdyaeva, S. K. Mahatha, M. Papagno, J. Sánchez-Barriga, O. Rader, L. Novinec, S. Gardonio and C. Carbone, Phys. Rev. B **91**, 195410 (2015).
[13] A. Varykhalov and O. Rader, Phys. Rev. B **80**, 035437 (2009).
[14] K. S. Kim, Y. Zhao, H. Jang, S. Y. Lee, J. M. Kim, K. S. Kim, J. -H. Ahn, P. Kim, J. -Y. Choi and B. H. Hong, Nature **457**, 706 (2009).
[15] E. Rollings, G. -H. Gweon, S. Y. Zhou, B. S. Mun, J. L. McChesney, B. S. Hussain, A. V. Fedorov, P. N. First, W. A. de Heer and A. Lanzara, J. Phys. Chem. Solids **67**, 2172 (2006).
[16] C. Hwang, D. Y. Kim, D. A. Siegel, K. T. Chan, J. Noffsinger, A. V. Fedorov, M. L. Cohen, B. Johansson, J. B. Neaton and A. Lanzara, Phys. Rev. B **90**, 115417 (2014).
[17] A. G. Rybkin, A. M. Shikin, D. Marchenko, A. Varykhalov and O. Rader, Phys. Rev. B **85**, 045425 (2012).
[18] A. H. Castro Neto, F. Guinea, N. M. R. Peres, K. S. Novoselov and A. K. Geim, Rev. Mod. Phys. **81**, 110 (2009).
[19] C. Hwang, C. -H. Park, D. A. Siegel, A. V. Fedorov, S. G. Louie and A. Lanzara, Phys. Rev. B **84**, 125422 (2011).
[20] H. Hwang and C. Hwang, J. Elec. Spectrosc. Relat. Phenom. **198**, 1 (2015).
[21] I. Gierz, J. Henk, H. Höchst, C. R. Ast and K. Kern, Phys. Rev. B **83**, 121408(R) (2011).